Aalborg Universitet

AALBORG UNIVERSITY

Thermal Analysis of Multi-MW Two-Level Generator Side Converters with Reduced Common-Mode-Voltage Modulation Methods for Wind Turbines

Qin, Zian; Liserre, Marco; Blaabjerg, Frede

Aalborg University

Thermal Analysis of Multi-MW Two-Level Generator Side Converters with Reduced Common-Mode-Voltage Modulation Methods for Wind Turbines

Zian Qin, Marco Liserre, Frede Blaabjerg
Center of Reliable Power Electronics (CORPE)
Department of Energy Technology, Aalborg University
Pontoppidanstraede 101, DK-9220 Aalborg East, Denmark
zqi@et.aau.dk, mli@et.aau.dk, fbl@et.aau.dk

Abstract – **Thermal performance influences both the cost of cooling system and the reliability of the power converter. Moreover, common-mode voltage in a generator drive may damage the bearing of the generator and also cause failure in a longer term. Therefore, both the thermal performance and common-mode voltage of the converter should be taken into account during the selection process of the modulation strategy. In this paper, two modulation strategies developed to reduce the common-mode-voltage reduced are compared based on the generator side converter of a 3 MW wind power system using the conventional-60° discontinuous PWM, where the common-mode voltage, power losses and thermal performance are all taken into account. The junction temperature and temperature of the power devices in the converter are obtained based on the thermal model by simulations and compared between the two modulation strategies.**

Keywords - **Modulation strategy; common-mode voltage; thermal performance; wind power converter**

I. INTRODUCTION

The modern wind power technology has developed very fast during the last decades and power electronics plays more and more critical role [1-4]. In large scale Wind Turbine Systems (WTS), the thermal performance of the power converter is becoming a critical indicator because of two main reasons: 1. complexity and cost of the cooling system will increase the cost of the converter; 2. the thermal excursion in the power device may accelerate its failure [5-7]. The power module's failure mechanism is caused by the fatigue of the solder joints between the different layers with different thermal expansion coefficients. Actually, both the mean temperature and temperature swing have impact on the lifetime of the power devices, which have been considered in Coffin-Manson-Arrhenius Model and verified by experiments [6], [7]. Thus, the lifetime of power converters can be evaluated and improved by thermal-oriented investigation as well as a good understanding of the mission profile combined with robust design [8]. Three-level neutral point clamped back-to-back converter topology, which achieves smaller size of filters and higher voltage handling capability, is a good choice in large scale wind power application, but the unequal thermal

performance between the outer and inner switching devices in a switching arm might reduce lifetime of power switching devices [8]. Power fluctuations may also cause thermal excursion in power converter, while reactive power can be pushed to reduce it [9]. Optimization of the modulation strategies may be used to improve the reliability of the power converter. The impact of different modulation strategies on thermal performance of the power converter has been compared and the Conventional-60° Discontinuous PWM (CONV-60° DPWM) was found to be the most optimal in power losses and thermal aspect [10], [11]. But Common-Mode (CM) Voltage in the power converter was not considered at all.

The CM voltage in the power converters may cause CM current between the converters and ground, which would lead to safety issues [12], [13]. In fact, in generators the CM current may induce failure of the bearings and thereby also reduce the reliability of the system [13]. Thus, the CM voltage caused by modulation strategies was investigated and it was found that common-mode voltage could be reduced if no zero vectors were applied in the modulation strategies [14-16]. Among the CM voltage reducing modulation strategies, the active zero state PWM (AZSPWM) and near state PWM (NSPWM) were found to be the most feasible.

Therefore, the scope of this paper is to investigate the thermal performance of the CM voltage reduced modulation strategies, AZSPWM and NSPWM, by comparing them with the CONV-60° DPWM. In section II a 3 MW Permanent Magnet Synchronous Generator (PMSG) based WTS with a single stage gearbox is modelled. In section III the CM voltages are compared both in time domain and frequency domain between the different PWM methods. The loss distribution in the power converter is investigated in Section IV. Finally, a thermal model is established and thermal performance of the power converter with different modulation strategies is compared in Section V.

II. WIND POWER SYSTEM MODEL

The thermal performance evaluation of the generator side converter is based on the optimal concept of WTS, which

utilizes not only a full-scale power converter and a permanent magnet synchronous generator (PMSG), but also a single stage gearbox in order to improve the reliability and also avoid a large rotor diameter, as shown in Fig. 1. A two-level back-to-back converter, the preferred solution at 3 MW level, is chosen as the full-scale power converter. To the generator side, an active rectifier is employed for Maximum Power Point Tracking (MPPT) by regulating the rotational speed of the wind turbine. The aerodynamic and generator parameters of the WTS are obtained from [17] and they are listed in Table I.
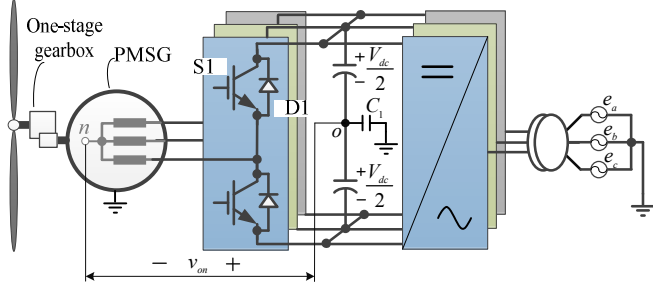

Fig.1. PMSG wind turbine system with a full-scale power converter.

TABLE I. WIND POWER SYSTEM PARAMETERS FOR 3 MW POWER LEVEL

Symbol	Name	Value
Aerodynamic parameters		
R	Blade radius	46.9 m
$V_{w,in}$	Cut-in wind speed	3 m/s
$V_{w,r}$	Rated wind speed	12.5 m/s
$V_{w,off}$	Cut-off wind speed	25 m/s
$C_{P,max}$	Maximum power coefficient	0.48
λ_{opt}	Optimal tip speed ratio	8.1
PMSG parameters		
n_r	Rated rotor speed	15 rpm
n_g	Gear ratio	6.36
N_P	Number of pole pairs	20
ψ_m	Magnetic induced flux	2.8 Wb
L_s	Stator inductance	0.18 mH

The DC-bus voltage is 1100 V, which is a common choice for WTS considering that the ac distribution line-to-line voltage is 690 V. The switching frequency f_s is fixed at 2 kHz and the maximum electrical frequency of the PMSG is 31.8 Hz. The control strategy is implemented in the synchronous d-q reference frame, as shown in Fig. 2. On q-axis, the outer loop is the rotational speed regulating the MPPT control, and the inner loop is the current control, which is actually related to the electromagnetic torque of the wind power generator. On the d-axis, the current reference $I_{s,d}^*$ is set to be zero in order to avoid damaging the magnetism of the generator. The pitch control will be applied to limit the power absorbed from wind, when wind speed is above the rated value for nominal power.
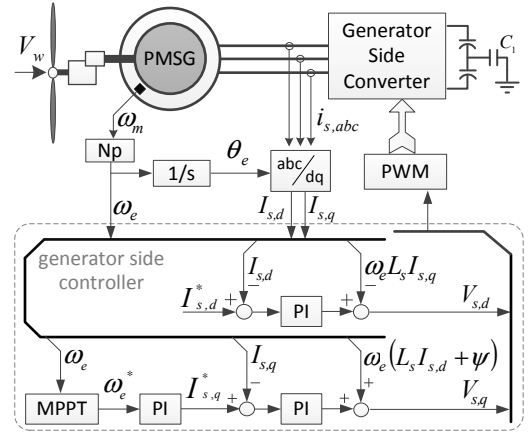

Fig. 2. Control diagram of the generator side converter.

III. REDUCED COMMON-MODE-VOLTAGE MODEULATION STRATEGIES

In a wind power generator the CM currents would flow through the parasitic capacitor between the inner ring and the outer ring of the bearing, and may damage the insulating layer between the two rings, thus the reliability of the system may be reduced. The circuit loop of the common-mode current in the wind power system is shown in Fig. 3, where v_{on} is the CM voltage of the PWM converter, L_s and r represent the equivalent stator impedance of the generator, C_1 is the grounded capacitor connected to the neutral point of the DC link and C_2 is the parasitic capacitor of the bearing. It should be noted that, so far the bearing currents in wind power generator have not been fully understood and besides the CM currents, the damaged rotor winding and some other issues are also included in the reasons of the bearing currents [18]. While in this paper, the focus is the CM currents caused by modulation methods, the path of which is only considered in Fig. 3.
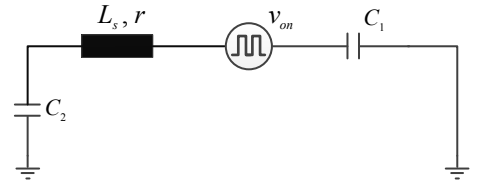
Fig. 3. Circuit loop of the common-mode current in wind power system.

It can be seen that the CM voltage of the PWM converter v_{on}, which is defined as the voltage between the neutral point of the dc link and that of the stator windings, is the only voltage source in the circuit. Therefore, it should be the main focus in order to reduce the bearing current. Compared with CM filters the relatively more cost-efficient approach is to optimize the modulation strategy, since it is one of the main causes of CM voltages. It was found that when zero switching vectors are applied in modulation methods, the amplitude of CM voltage will be $V_{dc}/2$, while without zero vectors, CM voltage would not be larger than $V_{dc}/6$. Therefore,

no zero vectors for reducing CM voltage modulation strategies were proposed [14], and the most feasible CM voltage reducing modulation methods are active zero state PWM and near state PWM, as indicated in Fig. 4.

(a) Active zero state PWM

(b) Near state PWM

Fig. 4. Voltage vectors of the reduced common-mode-voltage modulation methods.

A. Active Zero State PWM

The Active Zero State PWM (AZSPWM) method is similar to SVPWM method, which uses the two adjacent active vectors to synthesize the reference voltage, and the difference is that the AZSPWM method employs two 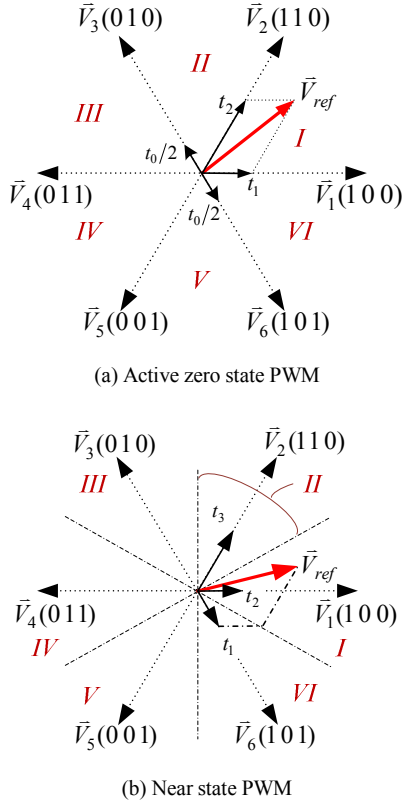opposite active vectors to synthesize zero vectors instead, as illustrated in Fig. 4(a). In the application of AZSPWM, the switches of the two phases would switch simultaneously in a short period, which will lead to sharply reversing the line-to-line voltage and be harmful to the machine. In order to avoid this issue, the modified AZSPWM (MAZSPWM) inserting zero-voltage time intervals between pulse reversals can be applied instead [15]. Since it is the same with AZSPWM theoretically, the simpler one - AZSPWM will be employed for analysis.

B. Near State PWM

The sectors of the Near State PWM (NSPWM) method are defined in another way, as seen in Fig. 4(b). The active vectors lie in the middle of the sectors, and three adjacent vectors are applied to synthesize the reference voltage. As it can be seen, in each sector the switches of one phase are kept open or
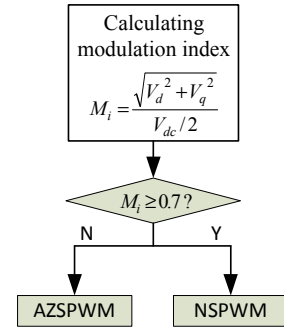
Fig. 5. Switching strategy of the combined AZSPWM+NSPWM method for reducing common-mode voltage.
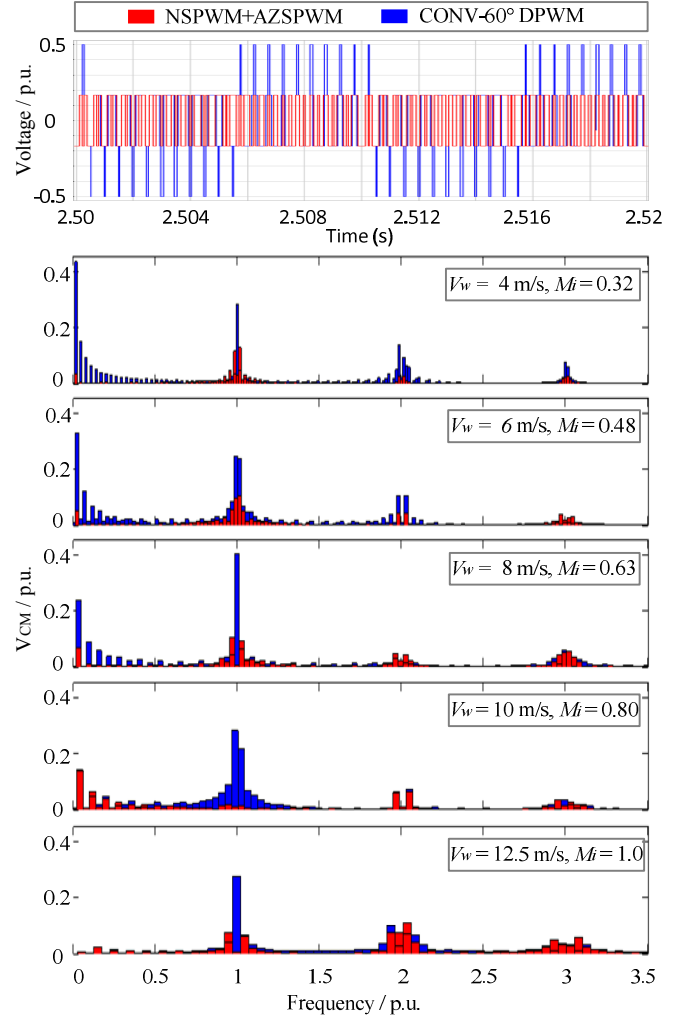
Note: $V_{dc} = 1$ p.u., $f_s = 1$ p.u.

Fig. 6. A comparison of the common-mode voltages and spectrum of the converter with different modulations at various wind speeds.

closed, which is similar to discontinuous PWM. It should be noted that since zero vectors cannot be synthesized by the three adjacent active vectors, NSPWM does only work at high modulation index, and the boundary is 0.67, where the modulation index M_i is defined as the ratio of the peak value of phase voltage and half of the dc bus voltage. Therefore,

NSPWM is combined with AZSPWM in order to control the variable speed wind turbine, as shown in Fig. 5.

A comparison of the CM voltages and spectrum of the converter with different modulations at various wind speeds is shown in Fig. 6. The upper part shows the CM voltages in the time domain. As mentioned before, the amplitude with NSPWM+AZSPWM is only 1/3 of that with CONV-60° DPWM. The lower part shows the spectrum of the CM voltages. Generally, the CM voltages with NSPWM+AZSPWM are much lower than with CONV-60° DPWM at the switching frequency especially at high wind speed. In details, when CONV-60° DPWM is applied, the CM voltage with low frequency will increase as the wind speed and modulation index decrease. However, the thing is different for NSPWM+AZSPWM: at high wind speed, where the modulation index is high and NSPWM is applied, CM voltages with low frequency are almost the same with that of CONV-60° DPWM, while at low wind speed, where the modulation index is low and AZSPWM is employed, CM voltages with low frequency are much lower than the CONV-60° DPWM.

IV. POWER LOSS MODELLING OF THE METHODS

In order to evaluate the thermal performance of the generator side converter, the power losses need to be calculated first. Assuming the three-phase loads of the converter are totally balanced, all the six switches of the converter would have the same power loss and thermal performance. Therefore, the power losses and temperature of S1 and D1, which are short for IGBT1 and Diode1 respectively, will be analyzed as representative of the generator side converter. Firstly, the power losses of the power devices are calculated by the model in [19], and the details are the following:

$$P_{loss} = P_{cond} + P_{sw} \tag{1}$$

For IGBT:

$$P_{cond,IGBT} = \frac{1}{T} \int_0^T V_{CE}(t) \cdot I_C(t) \cdot dt \tag{2}$$

$$P_{sw,IGBT} = \frac{1}{T} \sum_{k=0}^n (E_{on}(k) + E_{off}(k)) \tag{3}$$

For Diode:

$$P_{cond,Diode} = \frac{1}{T} \int_0^T V_F(t) \cdot I_F(t) \cdot dt \tag{4}$$

$$P_{sw,Diode} = \frac{1}{T} \sum_{k=0}^n E_{off}(k) \tag{5}$$

where P_{loss} is the total losses of the power device, P_{cond} is the conduction loss, P_{sw} is the switching loss, V_{CE} is the on-state voltage drop of the IGBT, I_C is the collector current of the IGBT, V_F is the forward voltage drop of the diode, I_F is the forward current of the diode, E_{on} is the switching-on energy loss, E_{off} is the switching-off energy loss, T is the period of the mean power losses and n is the switching cycles number of the power device in time T.

The data regarding the power losses of the power devices can be obtained in the product datasheet from the

manufacturer, and in this application, the power modules employed in the generator side converter are the HiPak IGBT Modules 5SNA 3600E170300 from ABB. Fig. 7 reveals both conduction loss and switching loss of the power devices using NSPWM in the time domain. As shown, in sector IV the S1 has neither conduction loss nor switching loss since it is closed, while in sector I, D1 has no switching loss but conduction loss as the complementary IGBT in the same phase with S1 is closed. These behaviors are quite similar to that of discontinuous PWM in time domain. Moreover, the instantaneous conduction loss and switching loss of S1 is higher than those of D1, but since the conduction time of D1 is longer than that of S1, the average power loss of the former one is higher, which is validated by Fig. 8.
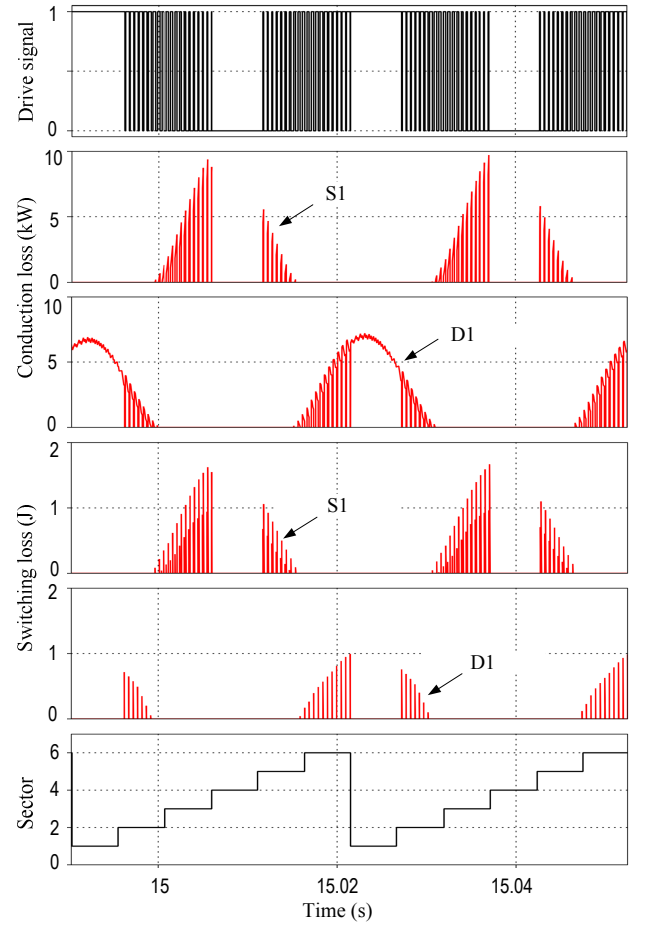
Fig. 7. Switching loss and conduction loss of the converter with NSPWM in different sectors.

Fig. 8 shows the comparison of the power loss distribution of the power device at various wind speeds. At high wind speed, the power loss of NSPWM is almost the same with that of CONV-60° DPWM, while at low wind speed, where the modulation method is transferred from NSPWM to AZSPWM, the power loss of CONV-60° DPWM is relatively lower. Moreover, the conduction loss is dominant in D1, while the switching loss is dominant in IGBT1. The power losses of the

converter at wind speed above 12.5 m/s are the same with that of 12.5 m/s, therefore they are not shown.

Fig. 8. Power loss distribution of the converter with different modulation schemes at various wind speeds.

V. THERMAL PERFORMANCES OF THE CONVERTER

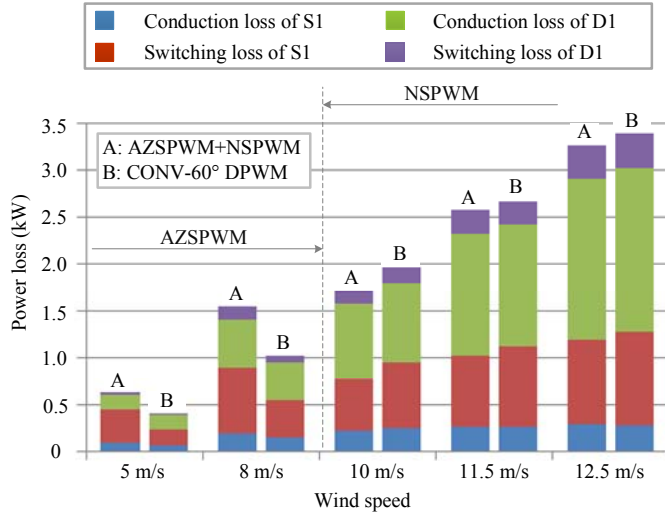Thermal cycling is one of the main drivers for failure of IGBT modules, since it can accelerate the fatigue of the solder joints between the different layers of the IGBT modules, which typically have different thermal expansion coefficients. Actually, in an IGBT module, the temperatures of the various solder joints are not the same, and their impacts on the lifetime of the IGBT module are also different [7]. However, as the purpose of this research is to compare the two modulation strategies in the thermal aspect, it is sufficient only to consider the junction temperature of the chip, which is relatively easier to be obtained by simulations. The thermal model of the IGBT module from the junction temperature to the ambient temperature sharing the same idea in [9] is shown in Fig. 9. Power loss of the device is considered to be a current source, and the temperature difference is similar to the voltage drop on the thermal impedance between the different parts of the power module. The thermal impedance from junction to case is defined by a four-layer foster RC network, as shown in Fig. 10, and the value of the thermal parameters of the power device can be acquired in the product datasheet from the manufacturer, which has been mentioned in section IV and listed in Table II. The thermal impedance from the case to heat sink is simplified as a thermal resistance and for S1 and D1 they are set to be 0.003 K/W and 0.006 K/W respectively by experience. The thermal impedance from heatsink to ambient $Z_{th(h-a)}$ is complex to be modelled, because it is related to the volume, material and shape of the heatsink. Furthermore, whether air cooling or water cooling is applied it has also a large impact on $Z_{th(h-a)}$. In fact, the thermal capacitance of the heat sink is much larger than that of the power devices, and since the purpose is in order to find the relatively better modulation strategies in thermal aspect, the thermal impedance

$Z_{th(h-a)}$ is ignored and the temperature of the heatsink T_h is assumed to be constant at 50℃.
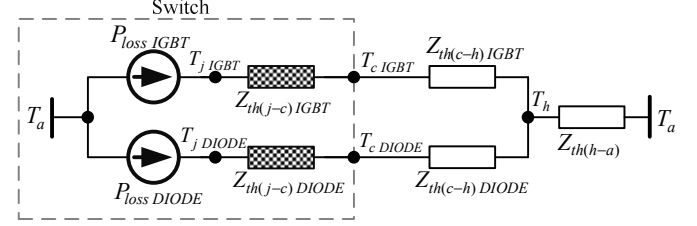
Note:
T_a : ambient temperature
T_j : junction temperature
T_c : case temperature
T_h : heat sink temperature
$Z_{th(j-c)}$: thermal impedance from junction to case
$Z_{th(c-h)}$: thermal impedance from case to heat sink
$Z_{th(h-a)}$: thermal impedance from heat sink to ambient

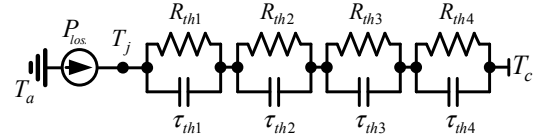Fig. 9. Thermal model of the converter.

Fig.10. Thermal impedance model of the power devices from junction to case.

TABLE II.   PARAMETERS OF THE THERMAL IMPEDANCE OF THE POWER DEVICES FROM JUNCTION TO CASE.

	i	1	2	3	4
IGBT	R_{thi} (K/kW)	5.059	1.201	0.495	0.246
	τ_{thi} (ms)	202.9	20.3	2.01	0.52
DIODE	R_{thi} (K/kW)	8.432	1.928	0.866	0.839
	τ_{thi} (ms)	210	29.6	7.01	1.49

Based on the thermal model mentioned above, the junction temperature with the two modulation strategies at full power rating is gained in time domain, as shown in Fig. 11. According to Fig. 8, at full power rating, NSPWM is employed in the hybrid modulation strategy. Therefore, both the mean junction temperature and temperature fluctuation of the power devices with NSPWM are almost the same with those of CONV-60° DPWM. In detail, the mean junction temperature of D1 is 87 ℃, and its temperature fluctuation is about 12 ℃. While the temperature of the S1 is much lower, where the mean junction temperature is 63 ℃ and the temperature fluctuation is around 6.5 ℃.

As it is seen in Fig. 12 both the mean junction temperature and the temperature fluctuation increase with the wind speed. However, when the wind speed is between the rated value and the cut-off speed, both the mean value and the fluctuation of the junction temperature are constant since the generating
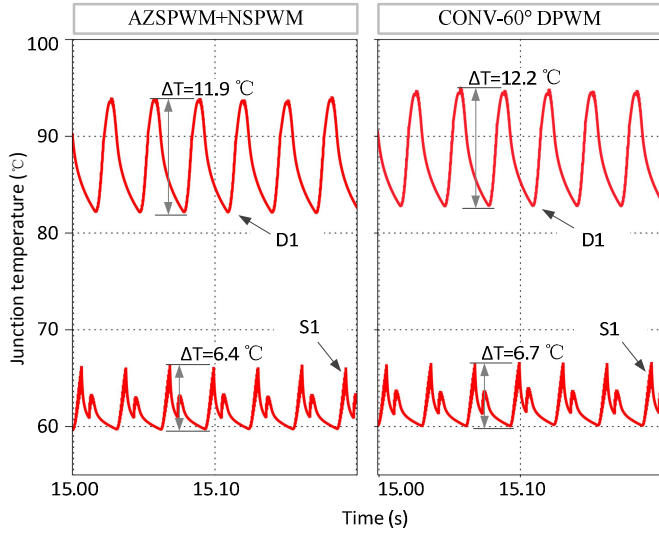
Fig. 11. Junction temperature of the power devices with different modulations at full power rating.
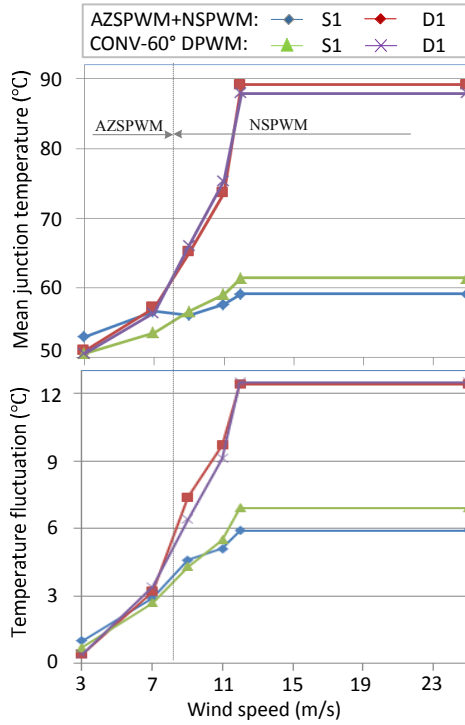

Fig. 12. Junction temperature of the chip with two modulation methods at different wind speeds.

power of the WTS is kept unchanged by pitch control as mentioned before. The diode has both higher mean junction temperature and temperature fluctuation compared to the IGBT, and the difference also increases with the wind speed. Moreover, at high wind speed, where the modulation index is high and NSPWM works in AZSPWM+NSPWM modulation strategy, the temperature of the IGBT is a little lower than that of CONV-60° DPWM, while at low wind speed, where the modulation index is also low and AZSPWM operates, the opposite result is observed.

VI. CONCLUSION

In large scale wind power application, the thermal performance and common-mode voltage of the generator side converter are two critical indicators. The former one is related to the cost of the cooling system and lifetime of the power devices, while the latter one may cause failure of the bearing in the wind generator. In this paper, based on the generator side converter of a 3 MW wind power system, the two most feasible common-mode voltage reduced modulation strategies, Active Zero State PWM and Near State PWM, are compared with the conventional-60° discontinuous PWM (CONV-60° DPWM), where the common-mode voltage, power losses and thermal performance are all taken into account. In detail, a 3 MW PMSG based wind power system with a single stage gearbox is modelled. Then, the common-mode voltages are compared both in time domain and frequency domain. The power loss distribution of the power converter with the two modulation strategies is analyzed. Finally, the thermal model of the power converter is established, and the junction temperature and temperature of the power devices in the converter are obtained by simulations and compared between the two modulation strategies. It can be concluded that both near state PWM and active zero state PWM have lower common-mode-voltage than CONV-60° DPWM, and near state PWM NSPWM has the same power losses and junction temperature with it, while AZSPWM has relatively higher power losses and junction temperature than CONV-60° DPWM. But since AZSPWM only works at low wind speed, where both the power and the mean temperature are low, it is not as critical as the performance of NSPWM, which works at high wind speed and high power. Therefore, the modulation strategy that using near state PWM combined with active zero state PWM is relatively more optimal to be applied in the generator side converter of a large scale wind power system from common-mode voltage and thermal aspect.

REFERENCES

[1] F. Blaabjerg, Z. Chen, and S. B. Kjaer, "Power electronics as efficient interface in dispersed power generation systems," *IEEE Trans. Power Electron.,* vol. 19, no. 5, pp. 1184–1194, Sep. 2004.

[2] Z. Chen, J. M. Guerrero, and F. Blaabjerg, "A review of the state of the art of power electronics for wind turbines," *IEEE Trans. Power Electron.,* vol. 24, no. 8, pp. 1859–1875, Aug. 2009.

[3] M. Liserre, R. Cardenas, M. Molinas, and J. Rodriguez, "Overview of multi-MW wind turbines and wind parks," *IEEE Trans. Ind. Electron.,* vol. 58, no. 4, pp. 1081–1095, Apr. 2011.

[4] F. Blaabjerg, M. Liserre, K. Ma, "Power electronics converters for wind turbine systems" *IEEE Trans. on Ind. Appl.,* vol.48, no.2, pp.708-719, 2012.

[5] C. Busca, R. Teodorescu, F. Blaabjerg, S. Munk-Nielsen, L. Helle, T. Abeyasekera, P. Rodriguez, "An overview of the reliability prediction related aspects of high power IGBTs in wind power applications," Microelectronics reliability, vol. 51, no. 9-11, pp. 1903-1907, 2011.

[6] H. Wang, K. Ma, F. Blaabjerg, "Design for reliability of power electronic systems," in Proc. of IECON' 2012, pp.33-44, 25-28 Oct. 2012.

[7] ABB Application Note, Load-cycling capability of HiPakTM IGBT modules, 2012.

[8] F. Blaabjerg, K. Ma, D. Zhou, "Power electronics and reliability in renewable energy systems," in Proc. of ISIE' 2012, pp.19-30, 28-31 May 2012.

[9] K. Ma, M. Liserre, F. Blaabjerg, "Reactive power influence on the thermal cycling of multi-MW wind power inverter," IEEE Trans. on Ind. Appl., vol.49, no.2, pp.922-930, 2013.

[10] A. Isidori, F. M. Rossi, F. Blaabjerg, "Thermal loading and reliability of 10 MW multilevel wind power converter at different wind roughness classes," in Proc. of ECCE' 2012, pp. 2172-2179, 15-20 Sept. 2012.

[11] F. Blaabjerg, F. A. Isidori, F. M. Rossi, "Impact of modulation strategies on power devices loading for 10 MW multilevel wind power converter," in Proc. of PEDG' 2012, pp. 751-758, 25-28 June 2012.

[12] T. Kerekes, M. Liserre, R. Teodorescu, C. Klumpner, M. Sumner, "Evaluation of Three-Phase Transformerless Photovoltaic Inverter Topologies," IEEE Trans. Power Electron., vol.24, no.9, pp.2202-2211, Sept. 2009.

[13] M. M. Swamy, K. Yamada, T. Kume, "Common mode current attenuation techniques for use with PWM drives," IEEE Trans. Power Electron., vol.16, no.2, pp.248,255, Mar 2001.

[14] A. M. Hava, E. U n, "Performance Analysis of Reduced Common-Mode Voltage PWM Methods and Comparison With Standard PWM Methods for Three-Phase Voltage-Source Inverters," IEEE Trans. Power Electron., vol. 24, no.1, pp. 241-252, Jan. 2009.

[15] A. M. Hava, E. U n, "A High-Performance PWM Algorithm for Common-Mode Voltage Reduction in Three-Phase Voltage Source Inverters," IEEE Trans. Power Electron., vol.26, no.7, pp.1998-2008, July 2011.

[16] D. Jiang, F. Wang, J. Xue, "PWM Impact on CM Noise and AC CM Choke for Variable-Speed Motor Drives," IEEE Trans. on Ind. Appl., vol. 49, no. 2, pp. 963-972, March-April 2013.

[17] H. Li, Z. Chen, H. Polinder, "Optimization of Multibrid Permanent-Magnet Wind Generator Systems," IEEE Trans. on Energy Conversion, vol.24, no.1, pp. 82-92, March 2009.

[18] K. Fischer, F. Besnard, L. Bertling, "Reliability-Centered Maintenance for Wind Turbines Based on Statistical Analysis and Practical Experience," IEEE Trans. On Energy Conversion, vol.27, no.1, pp.184-195, March 2012.

[19] F. Blaabjerg, U. Jaeger, S. Munk-Nielsen, "Power losses in PWM-VSI inverter using NPT or PT IGBT devices," IEEE Trans. Power Electron., vol.10, no.3, pp. 358-367, May 1995.